Global thermodynamic behavior of fluid mixtures in the critical region

G. X. Jin and S. Tang
Institute for Physical Science and Technology, University of Maryland, College Park, Maryland 20742

J. V. Sengers
Institute for Physical Science and Technology, University of Maryland, College Park, Maryland 20742
and Thermophysics Division, National Institute of Standards and Technology, Gaithersburg, Maryland 20899
(Received 6 August 1992)

In a previous publication [Z. Y. Chen, A. Abbaci, S. Tang, and J.V. Sengers, Phys. Rev. A **42**, 4470 (1990)] a renormalized Landau expansion was constructed for the thermodynamic free energy of one-component fluids that incorporates the crossover from singular thermodynamic behavior at the critical point to regular behavior far away from the critical point. In the present paper the approach is extended to obtain a crossover free energy for binary fluid mixtures in the region around the vapor-liquid critical line. The thermodynamic equations thus obtained are compared with experimental equation-of-state and specific-heat data for mixtures of carbon dioxide and ethane.

PACS number(s): 05.70.Ce, 05.70.Jk, 64.60.Fr

I. INTRODUCTION

The theoretical issues associated with the thermodynamic behavior of fluids near the vapor-liquid critical point have been developed in considerable detail. Asymptotically close to the critical point the thermodynamic properties satisfy scaling laws with universal critical exponents and universal scaling functions that are the same as those for the three-dimensional Ising model [1]. In recent years several attempts have been made to extend the asymptotic scaling laws by also including the effects from nonasymptotic critical fluctuations [2–5]. These efforts have led to the construction of a Helmholtz free energy that recovers the theoretically predicted scaling-law behavior asymptotically close to the critical point and incorporates the crossover to classical behavior far away from the critical point. It has been demonstrated that such a crossover Helmholtz free energy is capable of representing experimental thermodynamic-property data in a substantial range of temperatures and densities around the critical point [6–8].

The theoretical description of the thermodynamic properties of fluid mixtures in the vicinity of the vapor-liquid critical line is less well developed. In the case of binary fluid mixtures we have an additional degree of freedom. Since the molecules of nonionic fluid mixtures have short-range interactions, fluid mixtures still belong to the universality class of three-dimensional Ising-like systems. The asymptotic scaling laws for this universality class depend on only two relevant scaling fields, namely, a strong ordering field h conjugate to the order parameter and a weak temperaturelike field t. As a consequence it is concluded that the critical thermodynamic behavior of binary mixtures should be isomorphic to that of one-component fluids provided that an additional field ζ associated with the extra degree of freedom is kept constant. Some effects resulting from an additional degree of freedom were first pointed out by Fisher [9]. The application of the principle of critical-point universality to mixtures was elucidated in a systematic fashion by Griffiths and Wheeler [10]. Alternative approaches based on the same physical ideas were proposed by Saam [11] and Anisimov, Voronel, and Gorodetskii [12].

A specific model for the asymptotic thermodynamic behavior of fluid mixtures in the near-vicinity of the vapor-liquid critical line was first proposed by Leung and Griffiths [13]. Attempts have been made to use this model as a basis for representing thermodynamic-property data of mixtures of ^{3}He and ^{4}He [13], carbon dioxide and ethylene [14], and carbon dioxide and ethane [15], but only with modest success. Moldover and co-workers [16,17] have modified the Leung-Griffiths model to obtain a successful representation of pressures, densities, and surface tensions of many mixtures at vapor-liquid coexistence, as recently reviewed by Rainwater [18]. However, these results have not been extended to the one-phase region. Moreover, with a single exception [19], the applications of the Leung-Griffiths model have been in terms of so-called effective critical exponents [20] that differ from the true universal asymptotic exponent values. If one were to use the Leung-Griffiths model with the true universal critical exponents without introducing correction-to-scaling terms, the range of applicability of the model would become unrealistically small [21].

An alternative scaled equation of state for fluid mixtures in the vicinity of the critical line has been proposed by Anisimov and co-workers [22–24]. Their model does contain the true universal critical exponents and does include estimates for leading correction-to-scaling contributions. This model has recently been extended in an attempt to deal with the crossover to classical behavior [25]. However, this alternative approach has thus far been used to analyze specific-heat data of fluid mixtures only and a consistent representation of both equation-of-state and specific-heat data has not yet been demonstrated.

It is the purpose of the present paper to derive a thermodynamic free energy for fluid mixtures that not only incorporates the singular scaling-law behavior asymptotically close to the critical point, but also accounts for the crossover to classical behavior far away from the critical point. The goal is accomplished by extending to mixtures a crossover Helmholtz free-energy density previously obtained by Chen *et al.* for one-component fluids on the basis of a renormalized Landau expansion [6]. It will be shown that the resulting thermodynamic free-energy density obtained for mixtures is capable of representing both the pressure and the specific heat as a function of temperature, density, and concentration in a substantial region around the vapor-liquid critical line.

We shall proceed as follows. In Sec. II we describe the specific procedure adopted for mapping the thermodynamic surface of mixtures to that of one-component fluids following the ideas of Griffiths and Wheeler [10] and Leung and Griffiths [13]. In Sec. III we reformulate the crossover free-energy density previously obtained for one-component fluids in the critical region, and in Sec. IV we show how it can be applied to fluid mixtures. For mixtures the critical parameters are no longer constant, but they depend on the concentration. In Sec. IV we also discuss how the concentration dependence of the critical parameters is taken into account. The theoretical description developed in the present paper is restricted to fluid mixtures for which the critical points of the pure-fluid components are smoothly connected by a single critical line. In Sec. V a comparison is made with experimental equation-of-state and specific-heat data for mixtures of carbon dixoide and ethane. In Sec. VI we address some issues related to the choice of zero points of energy and entropy which are relevant for the representation of excess-enthalpy data. Some remaining problems are discussed in Sec. VII.

II. THERMODYNAMIC TRANSFORMATIONS

In formulating a thermodynamic surface for fluid mixtures we need to choose an appropriate set of thermodynamic variables. In accordance with the general considerations of Griffiths and Wheeler, one must make a distinction between "density variables," such as molar density and energy density, which are extensive thermodynamic properties taken per unit of volume V, and "field variables," which are intensive variables such as temperature T, pressure P, and chemical potential μ. The reason is that fields have identical values in the two coexisting phases, while densities have in general different values in coexisting phases. In the case of one-component fluids, appropriate independent field variables are $1/T$ and μ/T with P/T as a dependent field variable [1]. Hence, for mixtures near the vapor-liquid critical line it is natural to treat $1/T$, μ_1/T, and μ_2/T, where μ_1 and μ_2 are the chemical potentials of the two components, as independent field variables, while keeping P/T as a dependent field variable. In the case of one-component fluids the thermodynamic properties are made dimensionless with the aid of the critical parameters [1,6]. However, in the case of mixtures near the vapor-liquid critical line this procedure is no longer advantageous, since the critical parameters themselves are now functions of the concentration. Instead we follow Griffiths and Wheeler [10] by reducing μ_1/T and μ_2/T with the aid of the molar gas constant R:

$$\hat{\mu}_1=\frac{\mu_1}{RT}\ ,\quad \hat{\mu}_2=\frac{\mu_2}{RT}\ . \tag{2.1}$$

The corresponding temperature and pressure variables then become

$$\hat{T}=\frac{1}{RT},\quad \hat{P}=\frac{P}{RT}\ . \tag{2.2}$$

The variation of the dependent potential $\hat{P}$ as a function of the independent fields $\hat{T}$, $\hat{\mu}_1$, and $\hat{\mu}_2$ is given by

$$d\hat{P}=-\hat{u}\,d\hat{T}+\rho_1 d\hat{\mu}_1+\rho_2 d\hat{\mu}_2\ , \tag{2.3}$$

where $\hat{u}=U/V$ is the energy density, while ρ_1 and ρ_2 are the molar densities of the two components. Furthermore, the concentration x is defined as $x=\rho_2/\rho$, where $\rho=\rho_1+\rho_2$ is the total density.

Before proceeding let us digress briefly on the difference between a weak temperaturelike field and a strong ordering field. The specific heat measures the response to a temperature change and the susceptibility measures the response to a change of the chemical potential. For one-component fluids the specific heat c_V diverges weakly and the susceptibility χ diverges strongly. Hence, from the fluctuation-dissipation theorem it follows that the energy fluctuations will be much weaker than the density fluctuations, which become long range. Hence, the mass density is identified as the (asymptotic) order parameter and the chemical potential as the ordering field. In the case of a binary mixture there is still only one ordering field. In principle it could be either $\hat{\mu}_1$ or $\hat{\mu}_2$, while the other chemical potential would then act as a hidden field to be kept constant in mapping the binary mixture onto the one-component fluid. In general, any two analytic functions $h(\hat{\mu}_1,\hat{\mu}_2)$ and $\zeta(\hat{\mu}_1,\hat{\mu}_2)$ can be treated as ordering field and hidden field, but not all choices will be equally effective in practice. In the case of binary mixtures one commonly defines the hidden field $\zeta(\hat{\mu}_1,\hat{\mu}_2)$ in such a way that $0\le\zeta\le 1$, so that it effectively serves as a concentrationlike variable interpolating between the two pure-fluid limits [13]. The ordering field $h(\hat{\mu}_1,\hat{\mu}_2)$ is taken to be the field conjugate to the total density ρ, while the critical temperature $T_c(\zeta)$, density $\rho_c(\zeta)$, and pressure $P_c(\zeta)$ are now treated as functions of the hidden field ζ.

With these general guidelines in mind and noticing the presence of logarithmic singularities in $\hat{\mu}_1$ and $\hat{\mu}_2$ in the dilute mixture limits, we define the new field variables $h(\hat{\mu}_1,\hat{\mu}_2)$ and $\zeta(\hat{\mu}_1,\hat{\mu}_2)$ by

$$h=\ln(e^{\hat{\mu}_1}+e^{\hat{\mu}_2}),\quad \zeta=\frac{1}{1+e^{(\hat{\mu}_1-\hat{\mu}_2)}}\ , \tag{2.4}$$

so that

$$\hat{\mu}_1=h+\ln(1-\zeta),\quad \hat{\mu}_2=h+\ln\zeta\ . \tag{2.5}$$

In addition we define

$$\tau \equiv \frac{T - T_c(\zeta)}{T}, \quad \Delta\rho = \frac{\rho - \rho_c(\zeta)}{\rho_c(\zeta)} . \tag{2.6}$$

Substitution of (2.4)–(2.6) into (2.3) yields

$$d\hat{P} = \hat{U}\, d\tau + \rho\, dh + W\, d\zeta , \tag{2.7}$$

with

$$\hat{U} = \frac{\hat{u}}{RT_c(\zeta)} \tag{2.8}$$

and

$$W = \left[\frac{x}{\zeta} - \frac{1-x}{1-\zeta} \right] \rho + \hat{U} \frac{1}{T} \frac{dT_c}{d\zeta} . \tag{2.9}$$

The density W in (2.7), conjugate to the hidden field ζ, will not be of further interest here.

In order to apply the results previously obtained for the Helmholtz free-energy density of one-component fluids in the critical region [6], we need a thermodynamic free-energy density which contains the order parameter ρ as an independent variable. Such a thermodynamic potential is readily obtained by a Legendre transformation

$$\hat{A}_{\text{eff}} = h\rho - \hat{P} , \tag{2.10}$$

so that

$$d\hat{A}_{\text{eff}} = -\hat{U}\, d\tau + h\, d\rho - W\, d\zeta . \tag{2.11}$$

The thermodynamic free-energy density $\hat{A}_{\text{eff}}(\tau,\rho,\zeta)$ is closely related to, but not identical with, what is conventionally called the Helmholtz free-energy density. However, the advantage of introducing $\hat{A}_{\text{eff}}(\tau,\rho,\zeta)$ is that, at fixed ζ, $\hat{A}_{\text{eff}}$ has a critical point characterized by the parameters $T_c(\zeta)$, $\rho_c(\zeta)$, and $P_c(\zeta)$, and near this critical point $\hat{A}_{\text{eff}}$ should be isomorphic with the Helmholtz free-energy density of a one-component fluid near the critical point. That is, at constant ζ, $\hat{A}_{\text{eff}}$ will be the same (singular) function of τ and ρ as the Helmholtz free-energy density of a one-component fluid, with all system-dependent constants now depending parametrically on the hidden field ζ.

The actual experimental data are in practice obtained at constant concentration x and not at constant field ζ. The relationship between the concentration x and the hidden field ζ can be derived from [26]

$$x = \frac{\rho_2}{\rho} = \left[\frac{\partial \hat{P}}{\partial \hat{\mu}_2} \right]_{\hat{\mu}_1, \hat{T}} , \tag{2.12}$$

and one obtains

$$x = \zeta - \frac{\zeta(1-\zeta)}{\rho} \left[\left[\frac{\partial \hat{A}_{\text{eff}}}{\partial \zeta} \right]_{\tau,\rho} - \frac{1}{T} \frac{dT_c(\zeta)}{d\zeta} \left[\frac{\partial \hat{A}_{\text{eff}}}{\partial \tau} \right]_{\zeta,\rho} \right] . \tag{2.13}$$

We have thus a transformation from the physical variables T,ρ,x associated with experiments to the theoretical variables τ,ρ,ζ in terms of which the thermodynamic surface will be specified.

The transformation (2.4) from the original chemical potentials $\hat{\mu}_1$ and $\hat{\mu}_2$ to the new field variables h and ζ is similar to the transformation adopted by Leung and Griffiths [13] and by Moldover and Gallagher [16] and Rainwater [18,27], but there are some minor differences. First, the previous investigators defined the ordering field as $h - H(\zeta,\tau)$, where the function $H(\zeta,\tau)$ is chosen in such a way that the ordering field becomes zero on the vapor-liquid coexistence surface. However, the requirement that the ordering field become zero on the coexistence surface is only correct asymptotically [28] and is therefore no longer appropriate when one wants to include the full nonasymptotic critical behavior, as is done in the present paper. Furthermore, the implementation of this condition appears to be cumbersome in practice [27]. Another minor difference is that Rainwater advocates the use of T as the temperature variable rather than $1/RT$ as done in Refs. [2,3,6], as well as in the asymptotic equation of state originally proposed by Leung and Griffiths [13]. Arguments that $1/T$ is the more appropriate temperature variable have been presented in the literature [28–30].

III. CROSSOVER FREE ENERGY FOR ONE-COMPONENT FLUIDS

For one-component fluids Chen *et al.* have constructed a Helmholtz free-energy density that incorporates the crossover from singular behavior asymptotically close to the critical point to regular behavior far away from the critical point [6]. In terms of the quantities introduced in the preceding section, the pure components correspond to the limits $\zeta \to 0$ and $\zeta \to 1$. In these limits the Helmholtz free-energy density $\hat{A}$ is decomposed as

$$\hat{A}(\tau,\rho) = \frac{P_c}{RT_c} [\Delta \tilde{A}(\tau,\rho) + \tilde{A}_0(\tau) + \rho h_0(\tau)] , \tag{3.1}$$

where $\tilde{A}_0(\tau)$ and $h_0(\tau)$ represent analytic background contributions, which in practice are represented by truncated Taylor series expansions

$$\tilde{A}_0(\tau) = \sum_{j=0}^{4} \tilde{A}_j \tau^j , \tag{3.2}$$

$$h_0(\tau,\zeta) = \frac{1}{\rho_c} \sum_{j=0}^{5} \tilde{\mu}_j \tau^j , \tag{3.3}$$

with system-dependent coefficients $\tilde{A}_j$ and $\tilde{\mu}_j$. Since $\hat{A} - \rho(\partial \hat{A}/\partial\rho)_\tau = -\hat{P}$ in accordance with (2.10), it follows that

$$\tilde{A}_0 = -1 . \tag{3.4}$$

The term $\Delta\tilde{A}$ in (3.1) incorporates the effects of the long-range critical fluctuations. As shown by Chen *et al.* [6], it can be related to a renormalized Helmholtz free-energy density $\Delta\tilde{A}_r$ deduced from the Landau-Ginzburg-Wilson theory of critical phenomena by a transformation of the form

$$\Delta\tilde{A}(\tau,\rho)=\Delta\tilde{A}_r(t,M)-c\left[\frac{\partial\Delta\tilde{A}_r}{\partial M}\right]_t\left[\frac{\partial\Delta\tilde{A}_r}{\partial t}\right]_M , \quad (3.5)$$

with

$$t=c_t\tau+\left[\frac{\partial\Delta\tilde{A}_r}{\partial M}\right]_t \quad (3.6)$$

and

$$M=c_\rho(\Delta_\rho-d_1\tau)+c\left[\frac{\partial\Delta\tilde{A}_r}{\partial t}\right]_M . \quad (3.7)$$

In this transformation c_t and c_ρ are system-dependent coefficients that relate the Landau variables t and M to the physical variables τ and $\Delta\rho$, while c and d_1 are system-dependent constants related to vapor-liquid asymmetry. The term $\Delta\tilde{A}_r$ can be expressed in terms of a Landau expansion renormalized by a procedure originally developed by Nicoll and co-workers [31–33]. Specifically, Chen *et al.* obtained [6]

$$\begin{aligned}\Delta\tilde{A}_r(t,M)=&\tfrac{1}{2}tM^2\mathcal{T}\mathcal{D}+\frac{1}{4!}u^*\bar{u}\Lambda M^4\mathcal{D}^2\mathcal{U}\\&+\frac{1}{5!}a_{05}M^5\mathcal{D}^{5/2}\mathcal{V}\mathcal{U}\\&+\frac{1}{6!}a_{06}M^6\mathcal{D}^3\mathcal{U}^{3/2}+\frac{1}{4!}a_{14}tM^4\mathcal{T}\mathcal{D}^2\mathcal{U}^{1/2}\\&+\frac{1}{2!2!}a_{22}t^2M^2\mathcal{T}^2\mathcal{D}\mathcal{U}^{-1/2}-\tfrac{1}{2}t^2\mathcal{K} ,\end{aligned} \quad (3.8)$$

where $\bar{u}$, Λ, a_{05}, a_{06}, a_{14}, and a_{22} are system-dependent coefficients. The coefficient of the M^4 term in this expansion is written as $u^*\bar{u}\Lambda$, where Λ is a maximum cutoff wave number for the critical fluctuations [5,6] and u^* a fixed-point coupling constant [34]. The functions $\mathcal{T}$, $\mathcal{D}$, $\mathcal{U}$, $\mathcal{V}$, and $\mathcal{K}$ are rescaling functions defined by

$$\begin{aligned}&\mathcal{T}=Y^{(2-1)/\nu)/\omega},\quad \mathcal{D}=Y^{-\eta/\omega},\quad \mathcal{U}=Y^{1/\omega},\\&\mathcal{V}=Y^{(\omega_a-1/2)/\omega},\quad \mathcal{K}=\frac{\nu}{\alpha\bar{u}\Lambda}(Y^{-\alpha/\omega\nu}-1) ,\end{aligned} \quad (3.9)$$

where ν, η, and $\alpha=2-3\nu$ are the usual asymptotic critical exponents, while ω and ω_a are the critical exponents associated with the leading symmetric and asymmetric correction term [1,35]. The function Y is a crossover function to be determined from the set of coupled algebraic equations

$$1-[1-\bar{u}]Y=\bar{u}\left[1+\frac{\Lambda^2}{\kappa^2}\right]^{1/2}Y^{1/\omega} , \quad (3.10)$$

$$\kappa^2=t\mathcal{T}+\tfrac{1}{2}u^*\bar{u}\Lambda M^2\mathcal{D}\mathcal{U} . \quad (3.11)$$

The parameter κ is closely related to the inverse correlation length [3] and serves as a measure of the distance from the critical point [8]. In the asymptotic critical limit

$$\lim_{\Lambda/\kappa\to\infty}Y=\left[\frac{\kappa}{\bar{u}\Lambda}\right]^{\omega} , \quad (3.12)$$

and one recovers from (3.8) the asymptotic power laws with leading Wegner corrections [36]. The classical limit corresponds to

$$\lim_{\Lambda/\kappa\to 0}Y=1 , \quad (3.13)$$

so that (3.7) reduces to a classical Landau expansion.

The critical exponents and the fixed-point coupling constant u^* are universal. We continue to use the values earlier adopted by Chen *et al.* [6] and they are presented in Table I. The critical exponents ν, η, α, and ω are known with high accuracy [1,37]. The exponent ω_a of the asymmetric correction term is not well known [31,35,38]. The value $\omega_a=2.1$ is the one recommended by Zhang [39].

In addition to the critical parameters P_c, T_c, and ρ_c, the crossover free-energy density contains the following system-dependent constants: the crossover parameters $\bar{u}$ and Λ; the coefficients a_{05}, a_{06}, a_{14}, and a_{22} in the renormalized Landau expansion (3.8); the coefficients c_t, c_ρ, c, and d_1 in the relations (3.6) and (3.7) between the Landau variables; and the physical variables and the coefficients $\tilde{A}_j$ and $\tilde{\mu}_j$ in the expansions (3.2) and (3.3) for the background contributions. The critical parameters are either measured directly or deduced from an asymptotic analysis of available experimental data. With the exception of $\tilde{\mu}_j$, the system-dependent constants can be determined from a fit to experimental P-T-ρ data. The coefficients $\tilde{\mu}_j$ for $j\geq 2$ determine the background contributions to the caloric properties such as the specific heat or the sound velocity. The coefficients $\tilde{\mu}_0$ and $\tilde{\mu}_1$ fix the zero points of energy and entropy, and therefore do not enter into the calculation of thermodynamic properties such as the pressure and the specific heat.

In this paper we shall try to apply this crossover Helmholtz free-energy density to represent experimental equation-of-state and specific-heat data for mixtures of carbon dioxide and ethane. For the pure components the system-dependent coefficients have been previously determined by Chen *et al.* [6]. For carbon dioxide these coefficients were obtained from a comparison with P-ρ-T data of Michels and co-workers [40–42] and with c_V data of Edwards [43] supplemented with c_V values reported by Michels and de Groot [44]. For ethane these coefficients were obtained from a comparison with P-ρ-T of Douslin and Harrison [45] and with c_V data of Roder [46]. However, it was noted by Luettmer-Strathmann, Tang, and Sengers [47] that the caloric background thus obtained does not match well with the c_V values implied by a wide-range analytical equation for ethane recently pro-

TABLE I. Universal critical-region constants.

Constant	Value
ν	0.630
η	0.033 3
$\alpha=2-3\nu$	0.110
$\omega=\Delta/\nu$	0.809 52
ω_a	2.1
u^*	0.472

posed by Friend, Ingham, and Ely [48]. Hence, following Luettmer-Strathmann, Tang, and Sengers [47] we redetermined the caloric background parameters $\tilde{\mu}_j$ of ethane for $j \geq 2$ by making a comparison with the accurate c_V data of Shmakov close to the critical point [49] and supplementing them with c_V values calculated from the classical equation of Friend, Ingham, and Ely further away from the critical point. The c_V data obtained by Roder [46] are still represented with a standard deviation of 1.5%.

The values of the system-dependent constants for carbon dioxide and ethane are given in Table II. The values of the critical-point parameters T_c, ρ_c, and P_c of the two fluids are given in Table III. In this paper all temperatures refer to the International Practical Temperature Scale of 1968 (IPTS-68), since the previous analysis of Chen *et al.* for the two pure fluids used this temperature scale, while the new experimental data of Weber [50] for the mixture are also on IPTS-68.

The crossover model represents the experimental P-ρ-T in a range approximately determined by

$$\left[\frac{\partial^2 \Delta \tilde{A}}{\partial \Delta \rho^2}\right]_\tau \leq 2.2 \ . \tag{3.14}$$

This range is shown in Fig. 1 as a function of the reduced temperature variable $\Delta T^* = (T - T_c)/T_c$ and the reduced density variable $\Delta\rho = (\rho - \rho_c)/\rho_c$. It corresponds to

$$-0.05 \leq \Delta T^* \leq +0.29 \quad \text{at} \quad \rho = \rho_c \tag{3.15}$$

and

$$-0.60 \leq \rho \leq +0.70 \quad \text{at} \quad T = T_c \ . \tag{3.16}$$

A crucial test of any equation of state in the critical region is how well the equation represents caloric properties, such as the isochoric specific heat c_V, which is related to a second-order derivative of the Helmholtz free energy. Figure 2 shows a comparison with isochoric specific-heat data at $\rho = \rho_c$ obtained by Edwards for carbon dioxide [43] and Fig. 3 shows a comparison with isochoric specific-heat data at $\rho = \rho_c$ obtained by Shmakov for ethane [49]. The experimental c_V data of Edwards for CO_2, after the application of a correction for the heat capacity of the empty calorimeter as described by Al-

TABLE II. System-dependent constants.

Parameter	$k^{(1)}$ (Carbon dioxide[a])	$k^{(2)}$ (Ethane[a])	$k^{(m)}$
	Crossover parameters		
$\bar{u}$	0.398 03	0.369 10	0
Λ	1.421 4	1.121 6	0
	Scaling-field parameters		
c_t	1.955 1	1.555 8	−0.520
c_ρ	2.414 5	2.499 5	−0.174
c	−0.025 90	−0.028 92	0
d_1	−0.332 31	−0.363 55	0
	Classical parameters		
a_{05}	−0.270 63	−0.055 078	0
a_{06}	1.142 28	0.977 78	0
a_{14}	0.398 39	0.517 89	0
a_{22}	0.301 16	0.702 73	0
	Equation-of-state background parameters		
$\tilde{A}_1$	−6.007 9	−5.448 0	2.40
$\tilde{A}_2$	4.513 9	3.365 7	−1.63
$\tilde{A}_3$	−1.950 9	−1.402 2	1.35
$\tilde{A}_4$	5.137 1	10.49 9	0
	Caloric background parameters		
$\tilde{\mu}_2$	−13.730	−15.221	3.60
$\tilde{\mu}_3$	−7.919 1	−9.025 2	31.1
$\tilde{\mu}_4$	32.249	−3.209 2	−165.0
$\tilde{\mu}_5$	−93.274	−50.644	0
Molar mass	44.010	30.073	

[a]Reference [6].

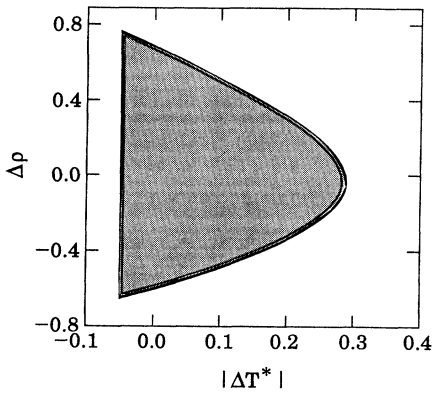

FIG. 1. Range of validity of the crossover free-energy density as a function of $\Delta T^* = (T - T_c)/T_c$ and $\Delta\rho = (\rho - \rho_c)/\rho_c$.

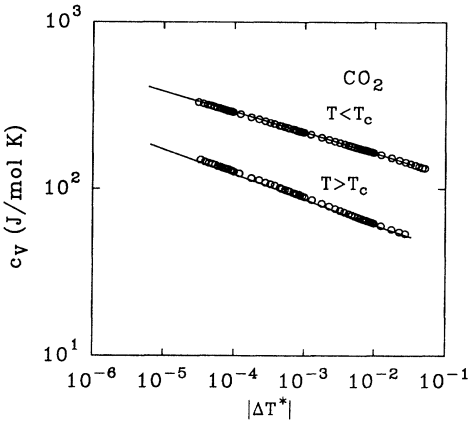

FIG. 2. Double-logarithmic plot of the isochoric specific heat c_V of carbon dioxide at $\rho = \rho_c$ as a function of $\Delta T^* = (T - T_c)/T_c$. The circles indicate the experimental values obtained by Edwards [43] and the solid curves represent the values calculated from the crossover free-energy density.

TABLE III. Critical-line coefficients for $CO_2+C_2H_6$.

Temperature (K) (Std. dev. 0.17 K)

$T_c^{(1)}=304.127$, $T_c^{(2)}=305.330$

$T_1=-54.6413$, $T_2=-52.6117$, $T_3=+150.0669$, $T_5=-88.0684$

Density (mol/l) (Std. dev. 1.8%)

$\rho_c^{(1)}=10.63$, $\rho_c^{(2)}=6.870$, $v_1=0.006\,621$, $v_2=0.048\,67$

Pressure (MPa mol/kJ) (Std. dev. 0.34%)

$P_c^{(1)}/RT_c^{(1)}=2.9167$, $P_c^{(2)}/RT_c^{(2)}=1.9191$, $P_1=-0.390\,10$, $P_2=+0.239\,61$

bright *et al.* [51], are reproduced with a standard deviation of 1.6%. The experimental c_V data of Shmakov for C_2H_6 are reproduced with a standard deviation of 1.5%.

IV. CROSSOVER FREE ENERGY FOR MIXTURES

According to the principle of critical-point universality, the behavior of the free-energy density $\hat{A}_{\rm eff}$, defined by (2.10) for mixtures, should be isomorphic with the free-energy density $\hat{A}$ of one-component fluids provided that the hidden field variable ζ is kept constant. Thus, in analogy to (3.1), we decompose $\hat{A}_{\rm eff}$ as

$$\hat{A}_{\rm eff}(\tau,\rho,\zeta)=\frac{P_c(\zeta)}{RT_c(\zeta)}[\Delta\tilde{A}(\tau,\rho,\zeta)+\tilde{A}_0(\tau,\zeta)+\rho h_0(\tau,\zeta)]\ , \tag{4.1}$$

with

$$\tilde{A}_0(\tau,\zeta)=\sum_{j=0}^{4}\tilde{A}_j(\zeta)\tau^j\ , \tag{4.2}$$

$$h_0(\tau,\zeta)=\frac{1}{\rho_c(\zeta)}\sum_{j=0}^{5}\tilde{\mu}_j(\zeta)\tau^j\ . \tag{4.3}$$

We note that in accordance with (3.4)

$$\tilde{A}_0(\zeta)=-1\ . \tag{4.4}$$

The transformation (3.5) for the critical part $\Delta\tilde{A}$ now becomes

$$\Delta\tilde{A}(\tau,\rho,\zeta)=\Delta\tilde{A}_r(t,M,\zeta)-c(\zeta)\left[\frac{\partial\Delta\tilde{A}_r}{\partial M}\right]_{t,\zeta}\left[\frac{\partial\Delta\tilde{A}_r}{\partial t}\right]_{M,\zeta}\ , \tag{4.5}$$

with

$$t=c_t(\zeta)\tau+c(\zeta)\left[\frac{\partial\Delta\tilde{A}_r}{\partial M}\right]_{t,\zeta}\ , \tag{4.6}$$

$$M=c_\rho(\zeta)[\Delta\rho-d_1(\zeta)\tau]+c(\zeta)\left[\frac{\partial\Delta\tilde{A}_r}{\partial t}\right]_{M,\zeta}\ . \tag{4.7}$$

Finally, $\Delta\tilde{A}_r$ is again represented by a truncated Landau expansion (3.8):

$$\Delta\tilde{A}_r(t,M,\zeta)=\tfrac{1}{2}tM^2\mathcal{T}\mathcal{D}+\frac{1}{4!}u^*\bar{u}(\zeta)\Lambda(\zeta)M^4\mathcal{D}^2\mathcal{U}+\frac{1}{5!}a_{05}(\zeta)M^5\mathcal{D}^{5/2}\mathcal{V}\mathcal{U}+\frac{1}{6!}a_{06}(\zeta)M^6\mathcal{D}^3\mathcal{U}^{3/2}+\frac{1}{4!}a_{14}(\zeta)tM^4\mathcal{T}\mathcal{D}^2\mathcal{U}^{1/2}+\frac{1}{2!2!}a_{22}(\zeta)t^2M^2\mathcal{T}^2\mathcal{D}\mathcal{U}^{-1/2}-\tfrac{1}{2}t^2\mathcal{H}\ , \tag{4.8}$$

where the rescaling functions $\mathcal{T}$, $\mathcal{D}$, $\mathcal{U}$, $\mathcal{V}$, and $\mathcal{H}$ are still related to the crossover function Y by (3.9). This crossover function Y is now determined by the equations

$$1-[1-\bar{u}(\zeta)]Y=\bar{u}(\zeta)\left[1+\frac{\Lambda^2(\zeta)}{\kappa^2}\right]^{1/2}Y^{1/\omega}\ , \tag{4.9}$$

$$\kappa^2=t\mathcal{T}+\tfrac{1}{2}u^*\bar{u}(\zeta)\Lambda(\zeta)M^2\mathcal{D}\mathcal{U}\ . \tag{4.10}$$

Thus, at constant ζ, the expressions for $\tilde{A}_{\rm eff}(\tau,\rho,\zeta)$ are identical to the expressions presented in the preceding section for the Helmholtz free-energy density $\hat{A}(\tau,\rho)$ of one-component fluids. The only difference is that all the system-dependent coefficients are now to be treated as (analytic) functions of the hidden field ζ.

A general Landau-Ginzburg-Wilson theory of critical phenomena cannot predict the values of system-dependent constants such as the critical parameters; they are to be obtained from experimental data that yield these critical parameters as a function of the concentration x. In this paper we restrict ourselves to binary mixtures for which the critical points of the two pure components are smoothly connected by a single critical line. The critical parameters can then be represented by simple polynomials as a function of x and $1-x$. However, we need the critical parameters as a function of the variable ζ. As noted by many previous investigators [4,16,18,23,27,52,53], it is therefore convenient to adjust the hidden field ζ in such a way that $x=\zeta$ on the critical line, so that $T_c(\zeta)$, $\rho_c(\zeta)$, and $P_c(\zeta)$ can be identified with

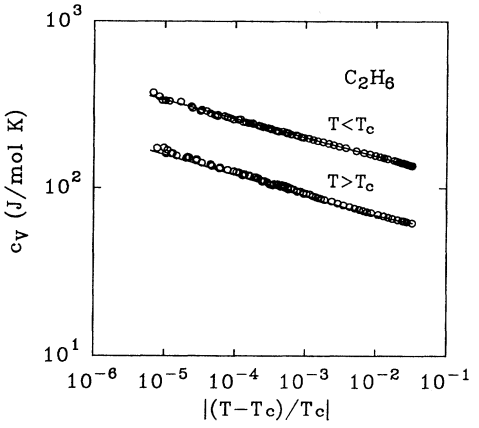

FIG. 3. Double-logarithmic plot of the isochoric specific heat c_V of ethane at $\rho=\rho_c$ as a function of $\Delta T^*=(T-T_c)/T_c$. The circles indicate the experimental values obtained by Shmakov [49] and the solid curves represent the values calculated from the crossover free-energy density.

$T_c(x)$, $\rho_c(x)$, and $P_c(x)$. On the critical line the $x(\zeta)$ transformation (2.13) reduces to

$$x=\zeta-\frac{\zeta(1-\zeta)}{\rho}G(\zeta)\ , \tag{4.11}$$

with

$$G(\zeta)=[\tilde{A}_0(\zeta)+\rho_c\tilde{\mu}_0(\zeta)]\frac{d(P_c/T_c)}{d\zeta}+\rho_c\frac{P_c}{T_c}\frac{d\tilde{\mu}_0(\zeta)}{d\zeta}-[\tilde{A}_1(\zeta)+\tilde{\mu}_1(\zeta)]\frac{P_c}{T_c^2}\frac{dT_c}{d\zeta}\ . \tag{4.12}$$

Obviously $x=\zeta$ on the critical line if we impose the condition

$$G(\zeta)=0\ . \tag{4.13}$$

We refer to (4.13) as the critical-line condition. In practice this condition is imposed by assigning specific functional forms to $\tilde{\mu}_0(\zeta)$ and $\tilde{\mu}_1(\zeta)$ so as to satisfy (4.13). In the pure-fluid limits $\zeta\to0$ and $\zeta\to1$ one can indeed assign arbitrary values to $\tilde{\mu}_0$ and $\tilde{\mu}_1$, but one does not have the thermodynamic freedom to impose arbitrary values for $\tilde{\mu}_0$ and $\tilde{\mu}_1$ at intermediate values of ζ. However, with prudence, this condition can be implemented approximately. Mathematically, there are an infinite number of solutions for (4.13). We choose the following solution:

$$\tilde{\mu}_0(\zeta)=\frac{\rho_c(\zeta)T_c(\zeta)}{P_c(\zeta)}\int_0^\zeta\frac{1}{\rho_c(x)}\frac{d}{dx}\left[\frac{P_c(x)}{T_c(x)}\right]dx\ , \tag{4.14}$$

$$\tilde{\mu}_1(\zeta)=-\tilde{A}_1(\zeta)\ . \tag{4.15}$$

The consequence of our procedure for implementing the critical-line condition (4.13) will be discussed in Sec. VI.

To determine the free-energy density $\hat{A}_{\rm eff}$ of the mixture completely, we also need to specify the ζ dependence of the system-dependent parameters $\bar{u}(\zeta)$, $\Lambda(\zeta)$, $c(\zeta)$, $c_t(\zeta)$, $c_\rho(\zeta)$, $d_1(\zeta)$, $a_{05}(\zeta)$, $a_{06}(\zeta)$, $a_{14}(\zeta)$, $a_{22}(\zeta)$, $\tilde{A}_1(\zeta)$, $\tilde{A}_2(\zeta)$, $\tilde{A}_3(\zeta)$, $\tilde{A}_4(\zeta)$, $\tilde{\mu}_2(\zeta)$, $\tilde{\mu}_3(\zeta)$, $\tilde{\mu}_4(\zeta)$, and $\tilde{\mu}_5(\zeta)$. For convenience we denote these system-dependent parameters by $k_i(\zeta)$, $i=1,\ldots,18$, and we need to interpolate them between the value $k_i(0)=k_i^{(1)}$ and $k_i(1)=k_i^{(2)}$ of the two pure components. For this purpose we adopt a simple interpolating equation of the form

$$k_i(\zeta)=k_i^{(1)}(1-\zeta)+k_i^{(2)}\zeta+k_i^{(m)}\zeta(1-\zeta)\ , \tag{4.16}$$

where $k_i^{(m)}$ are mixture coefficients.

Having specified the free-energy density $\hat{A}_{\rm eff}$ we obtain the ordering field h from

$$h=\left[\frac{\partial\hat{A}_{\rm eff}}{\partial\rho}\right]_{\tau,\zeta}\ . \tag{4.17}$$

The reduced pressure $\hat{P}=P/RT$ and the energy density $\hat{u}=U/V$ are obtained as

$$\hat{P}=\rho h-\hat{A}_{\rm eff}\ , \tag{4.18}$$

and

$$\hat{u}=-RT_c(\zeta)\left[\frac{\partial\hat{A}_{\rm eff}}{\partial\tau}\right]_{\rho,\zeta}\ . \tag{4.19}$$

One can deduce all other thermodynamic properties from $\hat{A}_{\rm eff}$ as well. The detailed expressions for the derivatives of $\hat{A}_{\rm eff}$ with respect to the density ρ and the reduced temperature τ are presented in the Appendix. For given T,ρ,x, the actual computation of the free-energy density $\hat{A}_{\rm eff}$ proceeds as follows:

(i) Take $\zeta_0=x$ as the initial estimate for ζ, and use (4.16) to calculate all the system-dependent coefficients of the mixture at $\zeta=\zeta_0$.

(ii) Use $t_0=c_t(\zeta_0)\tau$ and $M_0=c_\rho(\zeta_0)[\Delta\rho-d_1(\zeta_0)]$ as the zeroth-order estimates for t and M, respectively, and calculate the corresponding values $Y_0=Y(t_0,M_0)$ and $\kappa_0=\kappa(t_0,M_0)$ from (4.9) and (4.10) by iteration.

(iii) Use the Y_0 from (ii) to calculate $\Delta\tilde{A}_r$ from (4.8), and then calculate the first-order estimates t_1 and M_1 for t and M from (4.6) and (4.7).

(iv) Repeat (ii) and (iii) until convergence is obtained for t and M.

(v) Use the resulting t and M and the initial ζ_0 to calculate x' from (2.13). If $x'\neq x$, adjust the value of ζ until convergence is obtained.

(vi) The resulting ζ of the above procedures is thus the correct hidden variable that corresponds to the given T,ρ,x. Use this ζ to calculate $\Delta\tilde{A}_r(\tau,\rho,\zeta)$ and then the total free-energy density $\tilde{A}_{\rm eff}(\tau,\rho,\zeta)$ from (4.1)–(4.7).

V. APPLICATION TO MIXTURES OF CARBON DIOXIDE AND ETHANE

We have applied the crossover free-energy density derived in the preceding section to represent experimental equation-of-state data and specific-heat data of mixtures of carbon dioxide and ethane in the critical region. Attempts to represent thermodynamic-property data for this system in terms of a scaled equation of state have

been made by some previous investigators [15,16,23]. Moldover and Gallagher have analyzed vapor-liquid equilibrium data for mixtures of carbon dixoide and ethane [16]. Chang and Doiron have formulated an asymptotic scaled equation of state for the one-phase region near the critical line but in terms of empirical critical exponents [15]. The analysis of Anisimov, Kiselev, and Kostukova is restricted to specific-heat data only [23]. In the meantime an extensive set of experimental P-T-ρ-x data for mixtures of carbon dioxide and ethane has become available [50]. In addition, there exists a detailed set of isochoric specific-heat data measured by Shmakov [49].

In order to apply our theoretical free-energy density we need equations for the critical temperature T_c, the critical density ρ_c, and the critical pressure P_c as a function of the concentration x. The available experimental data for the critical parameters of mixtures of carbon dioxide and ethane have recently been evaluated by Abbaci *et al.* [54]. They are represented by polynomials of the form

$$T_c(x)=T_c^{(1)}(1-x)+T_c^{(2)}x + (T_1+T_2x+T_3x^2+T_4x^3)x(1-x)\ , \tag{5.1}$$

$$\frac{1}{\rho_c(x)}=\frac{1}{\rho_c^{(1)}}(1-x)+\frac{1}{\rho_c^{(2)}}x+(v_1+v_2x)x(1-x)\ , \tag{5.2}$$

$$\frac{P_c(x)}{RT_c(x)}=\frac{P_c^{(1)}}{RT_c^{(1)}}(1-x)+\frac{P_c^{(2)}}{RT_c^{(2)}}x+(P_1+P_2x)x(1-x), \tag{5.3}$$

where x is the molar concentration of ethane and where $T_c^{(i)}$, $\rho_c^{(i)}$, and $P_c^{(i)}$ are the critical parameters of carbon dioxide ($i=1$) and of ethane ($i=2$). The values of the coefficients T_j, v_j, and P_j in these equations are given in Table III. We prefer to consider Eqs. (5.2) and (5.3) for ρ_c^{-1} and $P_c(x)/RT_c(x)$, rather than equations for $\rho_c(x)$ and $P_c(x)$, so as to facilitate the implementation of condition (4.14). The critical temperature $T_c(x)$, the critical density $\rho_c(x)$ and the critical pressure $P_c(x)$ are shown in Fig. 4 as a function of x. The critical temperature $T_c(x)$ goes through a minimum at $x=0.436$. Furthermore, the system has a critical azeotrope at $x=0.281$. It should be noted that the critical parameters of the mixtures are known with considerably less accuracy than those of the pure fluids. Equations (5.1) and (5.2) represent the values of $T_c(x)$, $\rho_c^{-1}(x)$, and $P_c(x)/RT_c(x)$ with standard deviations of 0.18 K, 1.8%, and 0.35%, respectively. However, in evaluating the experimental data, Abbaci *et al.* had to make a number of adjustments to resolve discrepancies between values reported by various authors [54]. Even for a mixture as extensively investigated as $CO_2+C_2H_6$, there are inconsistencies of as much as 0.35 K for $T_c(x)$ and as much as 1.9% for $P_c(x)$ [54]. As a consequence of these uncertainties it will not be possible to represent experimental equation-of-state data of the mixtures with the same accuracy as previously obtained for pure carbon dioxide and ethane [6].

The crossover model for mixtures is now completely specified. The only adjustable parameters are the quadratic coefficients $k_i^{(m)}$ in Eq. (4.16). They are obtained from a fit to the P-ρ-T-x data obtained by Weber [50] and the $c_{V,x}$ data obtained by Shmakov [49]. Since the $c_{V,x}$ data reported by Shmakov cover a limited temperature range, we use, in addition, $c_{V,x}$ values far away from the critical line calculated from an analytic global equation of state recently developed by Ely and co-workers [55,56]. The coefficients $k_i^{(m)}$ represent deviations from a simple linear ξ dependence of the system-dependent coefficients $k(\xi)$. We only incorporated these corrections when they would lead to a substantial improvement in the standard deviations of the fit. As a consequence we only retained eight adjustable coefficients $k_i^{(m)}$ for the mixture, namely, in the equations for $c_\rho(\xi)$, $c_t(\xi)$, $\tilde{A}_1(\xi)$, $\tilde{A}_2(\xi)$, $\tilde{A}_3(\xi)$, $\tilde{\mu}_2(\xi)$, $\tilde{\mu}_3(\xi)$, and $\tilde{\mu}_4(\xi)$. The values of the eight coefficients $k_i^{(m)}$ are included in Table II.

When the pressure is calculated as a function of ρ, T, and x our crossover free-energy density reproduces the experimental pressure data of Weber [50] with a standard deviation of 0.6%. Experimental and calculated pressures as a function of temperature for a number of isochores are shown in Figs. 5–7. As mentioned above, the accuracy of the fit to the experimental P-ρ-T-x data is limited by the uncertainties in the critical-point parameters as a function of concentration. Specifically, at $x=0.748$ there exist some substantial discrepancies be-

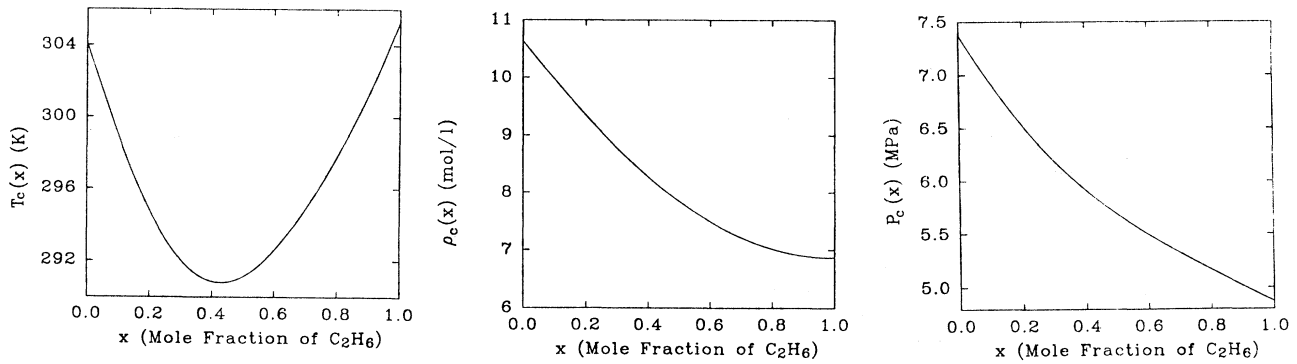

FIG. 4. The critical parameters $T_c(x)$, $\rho_c(x)$, and $P_c(x)$ of carbon dioxide and ethane mixtures as a function of the mole function x of ethane [54].

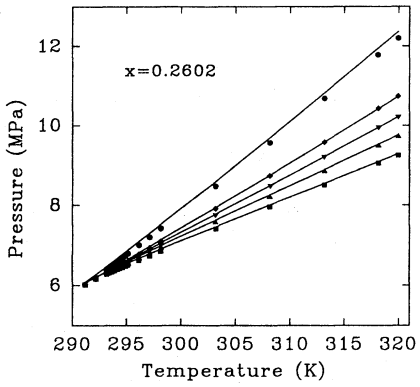

FIG. 5. Pressures of $CO_2+C_2H_6$ as a function of temperature for various densities at $x=0.2602$. The symbols indicate experimental pressures measured by Weber [50] and the curves represent pressures calculated from the crossover model (■, $\rho=7.3$ mol/l; ▲, $\rho=8.3$ mol/l; ▼, $\rho=9.1$ mol/l; ♦, $\rho=10.0$ mol/l; ●, $\rho=11.9$ mol/l).

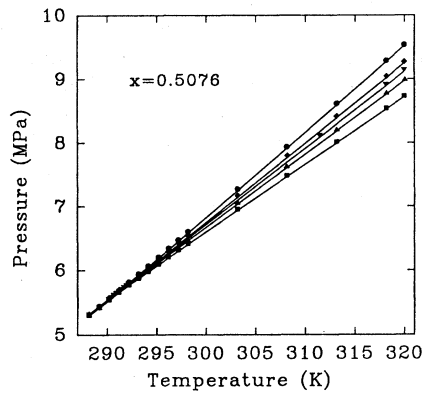

FIG. 6. Pressures of $CO_2+C_2H_6$ as a function of temperature for various densities at $x=0.5076$. The symbols indicate experimental pressures measured by Weber [50] and the curves represent pressures calculated from the crossover model (■, $\rho=7.1$ mol/l; ▲, $\rho=7.5$ mol/l; ▼, $\rho=7.8$ mol/l; ♦, $\rho=8.0$ mol/l; ●, $\rho=8.4$ mol/l).

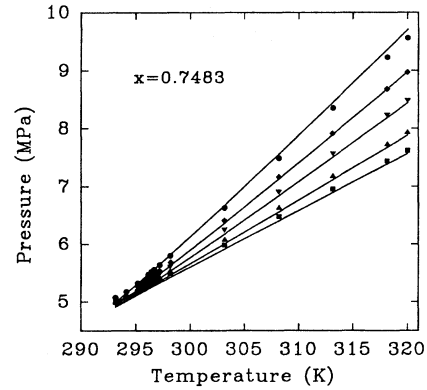

FIG. 7. Pressures of $CO_2+C_2H_6$ as a function of temperature for various densities at $x=0.7483$. The symbols indicate experimental pressures measured by Weber [50] and the curves represent pressures calculated from the crossover model (■, $\rho=6.5$ mol/l; ▲, $\rho=7.2$ mol/l; ▼, $\rho=8.2$ mol/l; ♦, $\rho=9.0$ mol/l; ●, $\rho=9.7$ mol/l).

tween the critical temperature and pressure deduced by Weber from his P-ρ-T-x data and those found by other investigators as represented by Eqs. (5.1) and (5.3) [54]. The origin of these discrepancies is not known.

Shmakov [49] has reported accurate $c_{V,x}$ data at $\rho=\rho_c(x)$ for mixtures of CO_2 and C_2H_6 at three compositions, namely, $x=0.281$, 0.436, and 0.720. As discussed in previous publications [6,8,54], there are some small discrepancies between the critical temperatures reported by Shmakov and those found by other investigators. Hence, we applied a shift of -0.0743 K at $x=0.281$, of $+0.0763$ K at $x=0.436$, and of $+0.0213$ K at $x=0.720$ to the temperatures attributed to the experimental $c_{V,x}$ data, so that the T_c values at these concentrations would coincide with those implied by Eq. (5.1). After this correction was applied our crossover Helmholtz free-energy density represents the experimental $c_{V,x}$ values at $x=0.281$, 0.436, and 0.720 with standard deviations of 1.1%, 1.6%, and 2.6%, respectively.

A comparison between the measured and calculated specific-heat values is shown in Figs. 8–10. The agreement at $x=0.281$ and $x=0.436$ is certainly within experimental accuracy. At $x=0.720$ there are some small discrepancies for the data very close to T_c, but two remarks should be made. First, as mentioned above, at this concentration there exists the largest uncertainty in the critical temperature and pressure [54], which may affect the equation of state implied by our Helmholtz free-energy density close to the critical line at this concentration. Second, Shmakov actually measured the ratio of an energy difference U_2-U_1 over a temperature difference T_2-T_1. At $x=0.720$, for some data points, he used temperature steps of $T_2-T_1\approx 0.035$, which are about four times larger than the temperature steps employed at the other concentrations and close to $T_c(x)$. These temperature differences are no longer small compared to $T-T_c(x)$. In comparing the experimental values with our crossover model we calculated the ratio of the corresponding energy and temperature differences, but the

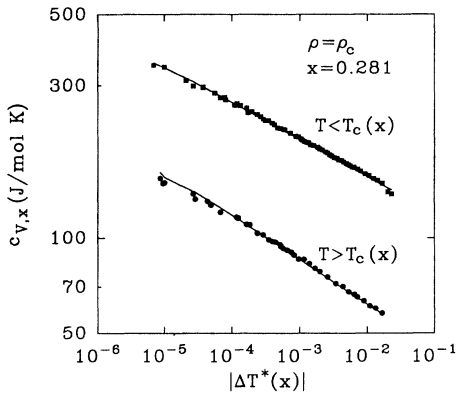

FIG. 8. Specific heat $c_{V,x}$ of $CO_2+C_2H_6$ at the critical density $\rho=\rho_c(x)$ as a function of $\Delta T^*(x)=[T-T_c(x)]/T_c(x)$ for $x=0.281$. The symbols indicate experimental data reported by Shmakov [49] and the curves represent values calculated from the crossover model.

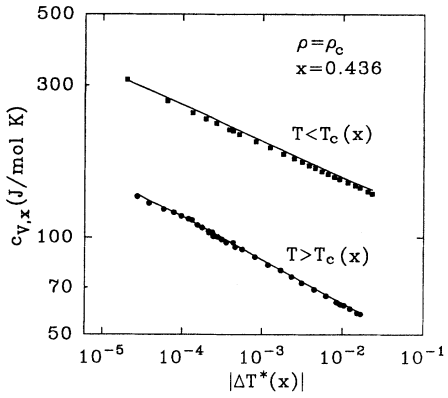

FIG. 9. Specific heat $c_{V,x}$ of $CO_2+C_2H_6$ at the critical density $\rho=\rho_c(x)$ as a function of $\Delta T^*(x)=[T-T_c(x)]/T_c(x)$ for $x=0.436$. The symbols indicate experimental data reported by Shmakov [49] and the curves represent values calculated from the crossover model.

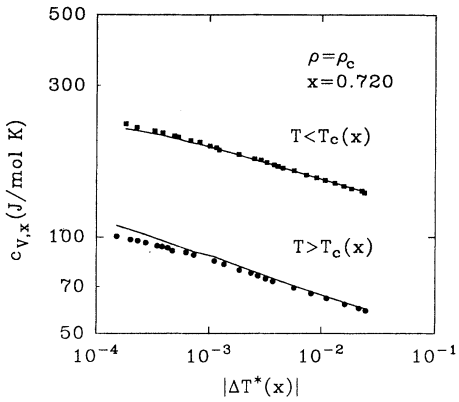

FIG. 10. Specific heat $c_{V,x}$ of $CO_2+C_2H_6$ at the critical density $\rho=\rho_c(x)$ as a function of $\Delta T^*(x)=[T-T_c(x)]/T_c(x)$ for $x=0.720$. The symbols indicate experimental data reported by Shmakov [49] and the curves represent values calculated from the crossover model.

question arises as to which temperatures the $c_{V,x}$ values thus obtained should be attributed [8]. In practice, we assigned the $c_{V,x}$ values not to the linear average but to the logarithmic average between T_1 and T_2. However, even this procedure may become less reliable when T_2-T_1 becomes comparable to $T-T_c(x)$.

The experimental specific-heat data obtained by Shmakov [49] cover a very limited range of temperatures. The specific heat in a larger temperature range is shown in Fig. 11. It can be seen that the $c_{V,x}$ values calculated from our Helmholtz free-energy density cross over to the values calculated from the global analytic equation of state developed by Magee, Howley, and Ely [56] at temperatures far away from the critical temperature. In principle we expect the coefficients $k_i^{(m)}$ in Eq. (4.16) for the system-dependent parameters $k_i(\zeta)$ to be of order unity. From the values quoted in Table II we see that this is indeed the case except for the coefficients $\tilde{\mu}_3^{(m)}$ and $\tilde{\mu}_4^{(m)}$. The latter coefficients are related to the temperature dependence of the background specific heat far away from the critical temperature and they are likely affected by the expected limited accuracy of the specific heat implied by the global analytic equation of state. Values of the pressure P, of the specific heat $c_{V,x}$, and of the hidden field variable ζ, calculated from the crossover model at some selected concentrations, temperatures, and densities, are presented in Table IV as an aid for computer-program verification.

At each value of the hidden field ζ the range of validity of our crossover model is in principle comparable to that of the pure fluids, as shown in Fig. 1. However, in practice there are some additional limitations, since the P-ρ-T-x data of Weber and $c_{V,x}$ data of Shmakov, which were used in determining the system-dependent coefficients, cover a more limited range. This limitation can only be partially remedied by including $c_{V,x}$ values calculated from another equation of state. Furthermore, at each concentration the P-ρ-T-x data of Weber were all obtained in the one-phase region with very few data points at temperatures below $T_c(x)$. As a consequence, our crossover equation will still have limited validity near the

TABLE IV. Table for computer verification.

Mole fraction of C_2H_6	ζ	Temperature (K)	Density (mol/l)	Pressure (MPa)	$c_{V,x}$ (J/mol K)	Phase region
0.281	0.283	287.39	8.879	5.606	145.13	2
0.281	0.282	291.45	8.879	6.119	175.92	2
0.281	0.281	293.93	8.879	6.455	67.74	1
0.281	0.282	297.00	8.879	6.878	57.95	1
0.436	0.431	284.01	8.463	5.066	139.01	2
0.436	0.435	291.61	8.463	5.937	72.42	1
0.436	0.436	292.43	8.463	6.042	66.33	1
0.436	0.438	295.37	8.463	6.422	58.22	1
0.720	0.711	288.14	6.938	4.596	142.78	2
0.720	0.717	292.68	6.938	5.018	158.39	2
0.720	0.722	295.48	6.938	5.294	109.06	1
0.720	0.727	302.27	6.938	6.000	60.08	1

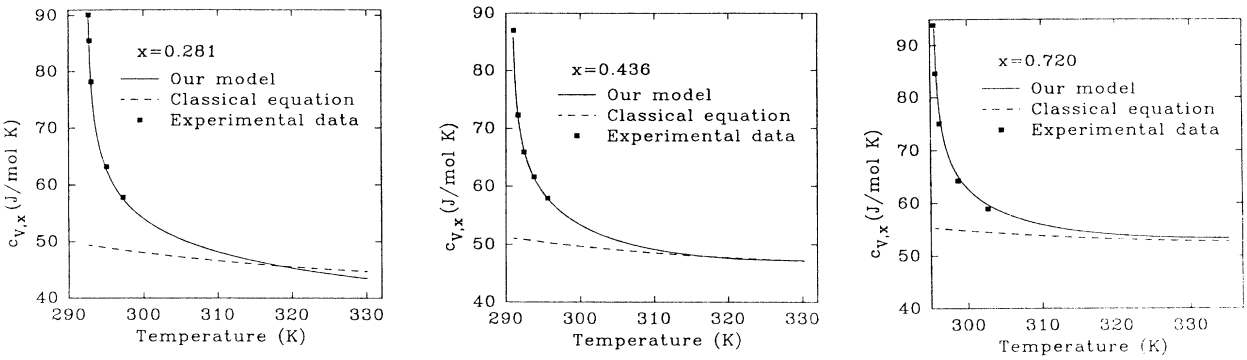

FIG. 11. Specific heat $c_{V,x}$ of $CO_2+C_2H_6$ at the critical density $\rho=\rho_c(x)$ as a function of temperature for $x=0.281$, 0.436, and 0.720. The squares indicate experimental data reported by Shmakov [49], the solid curves represent values calculated from the crossover model, and the dashed curves represent values calculated from the analytical equation of Magee, Howley, and Ely [56].

phase boundary at temperatures below $T_c(x)$.

Nevertheless we have calculated the vapor pressures and coexisting vapor and liquid densities implied by our crossover model. The calculated vapor and liquid densities are compared with experimental data reported by Khazanova, Lesnevskaya, and Zakharova [57] in Fig. 12. The agreement is comparable to that obtained by Moldover and Gallagher [16] and by Chang and Doiron [15] in terms of a scaled equation with effective empirical critical exponent values. The calculated vapor pressures are compared with experimental data reported by Khazanova, Lesnevskaya, and Zakharova [57] in Fig. 13 and with experimental data reported by Ohgaki and Katayama [58] in Fig. 14. For large values of the mole fraction x of ethane the agreement is comparable to that obtained by Moldover and Gallagher [16] and by Rainwater [59], but for $x \leq 0.5$ the agreement is not satisfactory. However, the figures also reveal the existence of appreciable discrepancies in the pure-fluid limits $x \to 0$ and $x \to 1$. Since our crossover model represents the P-ρ-T data of pure fluids [6,8], we conclude that there are inconsistencies between the data reported by Khazanova, Lesnevskaya, and Zhakarova and Ohgaki and Katayama for the mixture and those reported by other investigators for the pure fluids.

VI. ZERO POINT OF ENERGY AND HEAT OF MIXING

In developing our crossover model we have implemented the critical-line condition (4.13) by selecting the coefficients $\tilde{\mu}_0(\zeta)$ and $\tilde{\mu}_1(\zeta)$ in accordance with (4.14) and (4.15). Specifically, $\tilde{\mu}_1(\zeta)$ was identified with $-\tilde{A}_1(\zeta)$, while $\tilde{\mu}_0(\zeta)$ was determined by integrating (4.14). In Fig. 15 we show $\tilde{\mu}_0(\zeta)$ as a function of ζ. It is seen that the dependence of $\tilde{\mu}_0(\zeta)$ on ζ shows only small deviations from a linear variation.

On the critical line $x=\zeta$ the coefficients $\tilde{\mu}_0(x)$ and $\tilde{\mu}_1(x)$ are related to the internal energy density $\hat{u}=u/V$ and entropy density $\hat{s}=S/V$ by

$$\hat{u}_c(x)=P_c(x)[\tilde{A}_1(x)+\tilde{\mu}_1(x)] , \tag{6.1}$$

and

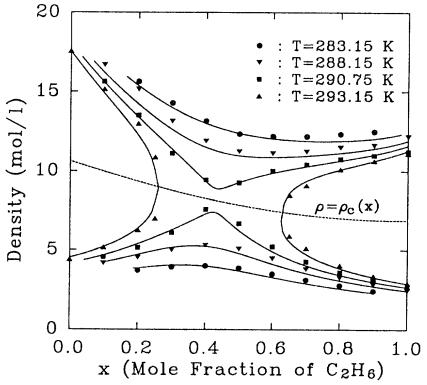

FIG. 12. The coexisting vapor and liquid densities of $CO_2+C_2H_6$ at various temperature as a function of the concentration x. The symbols indicate experimental values reported by Khazanova, Lesnevskaya and Zakharova [57] and the curves represent values calculated from the crossover model.

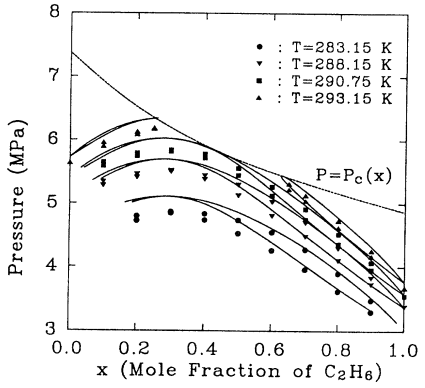

FIG. 13. The vapor pressure of $CO_2+C_2H_6$ at various temperatures as a function of the concentration x. The symbols indicate experimental values reported by Khazanova, Lesnevskaya, and Zakharova [57] and the curves represent values calculated from the crossover model.

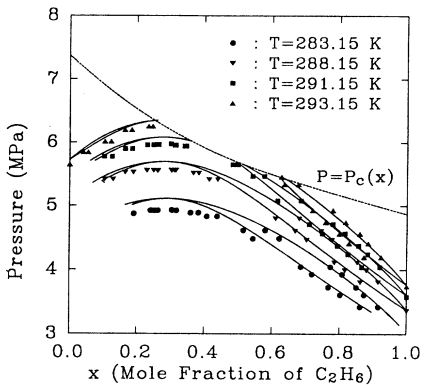

FIG. 14. The vapor pressure of $CO_2+C_2H_6$ at various temperatures as a function of the concentration x. The symbols indicate experimental values reported by Ohgaki and Katayama [58] and the curves represent values calculated from the crossover model.

$$\hat{s}_c(x)=\frac{P_c(x)}{T_c(x)}[1-\tilde{\mu}_0(x)-\tilde{A}_1(x)-\tilde{\mu}_1(x)] -R\rho_c(x)[x\ln x+(1-x)\ln(1-x)] . \quad (6.2)$$

Thus $\tilde{\mu}_1$ determines the zero point of energy and, for given $\tilde{\mu}_1$, $\tilde{\mu}_0$ determines the zero point of entropy. For the pure fluids these zero points or, equivalently, $\tilde{\mu}_0$ and $\tilde{\mu}_1$ can be chosen arbitrarily, but for the mixtures such a thermodynamic degree of freedom does not exist. Hence, in contrast to an earlier suggestion of Rainwater [27], the critical-line condition (4.13) introduces an approximation, even when the theoretical model is only used to represent P-ρ-T-x data [54].

In principle the critical-line condition can be implemented in many different ways [4,16,18,23,27,52,53,60]. The practical consequences of this approximation will depend on the specific manner in which the condition is implemented. From (4.15) and (6.1) we note that in our approach the critical-line condition is implemented by demanding that the internal energy is zero everywhere on the critical line.

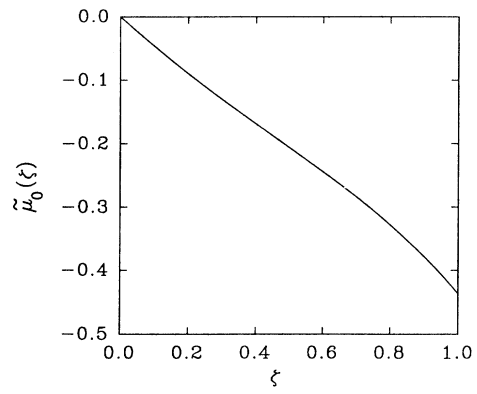

FIG. 15. The coefficient $\tilde{\mu}_0$ as a function of ζ as determined from Eq. (4.14). The dependence on ζ shows only small deviations from a linear variation.

As pointed out by Anisimov and Sengers [60], the critical-line condition (4.13) puts a restriction on the relationship between the partial molar volumes and partial molar enthalpies and, hence, on the volume and heat of mixing on the critical line. Since we have fitted the theoretical Helmholtz free-energy density to experimental volume data measured by Weber [50], the effect of imposing the critical-line condition (4.13) can lead to a distortion of the heat of mixing near the critical line. Fortunately, Wormald and Hodgetts have recently obtained heat-of-mixing data for $CO_2+C_2H_6$ mixtures near the critical line [61]. A comparison between the measured and calculated values of the molar excess enthalpy H^E is shown is Fig. 16. It should be noted that the comparison can only be made with limited accuracy. The reason is that neither the experimental pressure data of Wormald and Hodgetts nor our fit to the pressure data of Weber is sufficiently accurate to calculate the densities associated with the experimental excess enthalpy data with satisfactory accuracy. Nevertheless, from the observation that our crossover model implies a heat of mixing near the critical line of the correct order of magnitude we expect that any distortion of our Helmholtz free-energy density due to the imposition of the condition $x=\zeta$ on the critical line will be small.

VII. DISCUSSION

We have developed a Helmholtz free-energy density for fluid mixtures near the vapor-liquid critical line that incorporates the asymptotic scaling laws with Ising critical exponent values and which can be shown to yield a consistent representation of both P-ρ-T-x and $c_{V,x}$ data. Moreover, the Helmholtz free-energy density obtained reduces to a regular analytic free-energy density far away from the critical line.

Nevertheless, in reaching this result we have encountered some problems of both a practical nature and a theoretical nature. From a practical point of view a more accurate test of the validity of our theoretical crossover Helmholtz free-energy density is hampered by inconsistencies between various experimental data sets, even for a mixture as well investigated as $CO_2+C_2H_6$. Among others, these discrepancies lead to some serious inaccuracies in our knowledge of the location of the critical locus [54]. In principle, we can obtain a better fit to the experimental pressure data reported by Weber [50] if the concentration dependence of the critical-point parameters $T_c(x)$, $\rho_c(x)$, and $P_c(x)$ would be represented by equations with freely adjustable parameters, as done in some previous studies [16,59]. However, it would increase the discrepancy of our Helmholtz free-energy density with experimental data of other investigators [54]. A theoretical limitation is the condition that the hidden field variable ζ be equal to the concentration x on the critical line. We have argued that the manner in which we have implemented this condition does not lead to a significant distortion of the equation obtained for the calculation of pressure and specific-heat values. However, for an accurate representation of excess functions it will be desirable

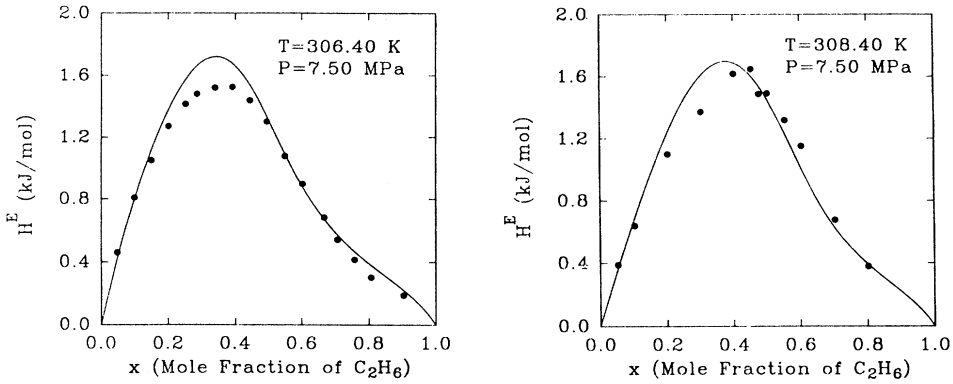

FIG. 16. The molar excess enthalpy H^E of $CO_2+C_2H_6$ at $P=7.50$ MPa and $T=306.40$ K and $T=308.40$ K. The circles indicate experimental values obtained by Wormald [61] and the curves represent values calculated from the crossover model.

to drop the critical-line condition at the expense of some added complexity in the use of the crossover model.

At this stage our crossover model for the Helmholtz free-energy density is primarily suited for representing the thermodynamic properties of mixtures in the one-phase region near the critical line. We have not yet been able to include a representation of the vapor pressures and the densities of the vapor and liquid phases at the two-phase boundary of the same quality as obtained by Moldover and Gallagher [16] and Rainwater [59] with equations especially designed for the phase boundary. To improve the capability of our crossover Helmholtz free-energy density for dealing with properties in and near the two-phase region, additional research will be necessary.

ACKNOWLEDGMENTS

The authors are indebted to L. A. Weber and C. J. Wormald for providing their experimental data prior to publication and to A. Abbaci and Z. Y. Chen for valuable contributions in the initial stage of this research. The authors also acknowledge stimulating discussions with M. A. Anisimov, S. B. Kiselev, J. M. H. Levelt Sengers, J. Luettmer-Strathmann, and J. C. Rainwater. The research is supported by the Division of Chemical Sciences of the Office of Basic Energy Sciences of the U.S. Department of Energy under Grant No. DE-FG05-88ER13902.

APPENDIX

1. Fundamental thermodynamic quantities

$$\hat{T}=\frac{1}{RT},\quad \hat{P}=\frac{P}{RT},\quad x=\rho_2/\rho\ ,$$
$$\hat{u}=U/V,\quad \hat{\mu}_1=\frac{\mu_1}{RT},\quad \hat{\mu}_2=\frac{\mu_2}{RT}\ , \tag{A1}$$

with

$$d\hat{P}=-\hat{u}\,d\hat{T}+\rho_1 d\hat{\mu}_1+\rho_2 d\hat{\mu}_2\ . \tag{A2}$$

2. Isomorphic thermodynamic quantities

$$h=\ln(e^{\hat{\mu}_1}+e^{\hat{\mu}_2}),\quad \zeta=\frac{1}{1+e^{(\hat{\mu}_1-\hat{\mu}_2)}}\ , \tag{A3}$$

$$\tau\equiv\frac{T-T_c(\zeta)}{T},\quad \Delta\rho=\frac{\rho-\rho_c(\zeta)}{\rho_c(\zeta)}\ , \tag{A4}$$

$$\hat{U}=\frac{\hat{u}}{RT_c(\zeta)}\ , \tag{A5}$$

$$\hat{A}_{\rm eff}=h\rho-\hat{P}\ , \tag{A6}$$

with

$$W=\left[\frac{x}{\zeta}-\frac{1-x}{1-\zeta}\right]\rho+\hat{U}\frac{1}{T}\frac{dT_c}{d\zeta}\ , \tag{A7}$$

$$d\hat{P}=\hat{U}\,d\tau+\rho\,dh+W\,d\zeta\ , \tag{A8}$$

$$d\hat{A}_{\rm eff}=-\hat{U}\,d\tau+h\,d\rho-W\,d\zeta\ . \tag{A9}$$

The relation between x and ζ is

$$x=\zeta-\frac{\zeta(1-\zeta)}{\rho}\left[\left[\frac{\partial\hat{A}_{\rm eff}}{\partial\zeta}\right]_{\tau,\rho}-\frac{1}{T}\frac{dT_c(\zeta)}{d\zeta}\left[\frac{\partial\hat{A}_{\rm eff}}{\partial\tau}\right]_{\zeta,\rho}\right]\ . \tag{A10}$$

3. Equations for crossover model

$$\hat{A}_{\rm eff}(\tau,\rho,\zeta)=\frac{P_c(\zeta)}{RT_c(\zeta)}[\Delta\tilde{A}(\tau,\rho,\zeta)+\tilde{A}_0(\tau,\zeta)+\rho h_0(\tau,\zeta)]\ , \tag{A11}$$

with

$$\tilde{A}_0(\tau,\zeta)=-1+\sum_{j=1}^{4}\tilde{A}_j(\zeta)\tau^j\ , \tag{A12}$$

$$h_0(\tau,\zeta)=\frac{1}{\rho_c}\sum_{j=0}^{5}\tilde{\mu}_j(\zeta)\tau^j\ . \tag{A13}$$

The critical part $\Delta\tilde{A}$ is given by

$$\Delta\tilde{A}(\tau,\rho,\xi)=\Delta\tilde{A}_r(t,M,\xi)-c(\xi)\left[\frac{\partial\Delta\tilde{A}_r}{\partial M}\right]_{t,\xi}\left[\frac{\partial\Delta\tilde{A}_r}{\partial t}\right]_{M,\xi}, \tag{A14}$$

with

$$\Delta\tilde{A}_r(t,M,\xi)=\tfrac{1}{2}tM^2\mathcal{T}\mathcal{D}+\frac{1}{4!}u^*\bar{u}(\xi)\Lambda(\xi)M^4\mathcal{D}^2\mathcal{U}+\frac{1}{5!}a_{05}(\xi)M^5\mathcal{D}^{5/2}\mathcal{V}\mathcal{U}+\frac{1}{6!}a_{06}(\xi)M^6\mathcal{D}^3\mathcal{U}^{3/2}$$
$$+\frac{1}{4!}a_{14}(\xi)tM^4\mathcal{T}\mathcal{D}^2\mathcal{U}^{1/2}+\frac{1}{2!2!}a_{22}(\xi)t^2M^2\mathcal{T}^2\mathcal{D}\mathcal{U}^{-1/2}-\tfrac{1}{2}t^2\mathcal{H}, \tag{A15}$$

and

$$t=c_t(\xi)\tau+c(\xi)\left[\frac{\partial\Delta\tilde{A}_r}{\partial M}\right]_{t,\xi}, \tag{A16}$$

$$M=c_\rho(\xi)[\Delta\rho-d_1(\xi)\tau]+c(\xi)\left[\frac{\partial\Delta\tilde{A}_r}{\partial t}\right]_{M,\xi}. \tag{A17}$$

The rescaling functions $\mathcal{T}$, $\mathcal{D}$, $\mathcal{U}$, $\mathcal{V}$, and $\mathcal{H}$ are

$$\mathcal{T}=Y^{(2-1/\nu)/\omega},\quad \mathcal{D}=Y^{-\eta/\omega},\quad \mathcal{U}=Y^{1/\omega},$$
$$\mathcal{V}=Y^{(\omega_a-1/2)/\omega},\quad \mathcal{H}=\frac{\nu}{\alpha\bar{u}\Lambda}(Y^{-\alpha/\omega\nu}-1). \tag{A18}$$

The crossover function Y is to be determined from the equations

$$1-[1-\bar{u}(\xi)]Y=\bar{u}(\xi)\left[1+\frac{\Lambda^2(\xi)}{\kappa^2}\right]^{1/2}Y^{1/\omega}, \tag{A19}$$

$$\kappa^2=t\mathcal{T}+\tfrac{1}{2}u^*\bar{u}(\xi)\Lambda(\xi)M^2\mathcal{D}\mathcal{U}. \tag{A20}$$

The relevant thermodynamic derivatives are

$$\left[\frac{\partial\Delta\tilde{A}}{\partial\Delta\rho}\right]_{\tau,\xi}=c_\rho(\xi)\left[\frac{\partial\Delta\tilde{A}_r}{\partial M}\right]_{t,\xi}, \tag{A21}$$

$$\left[\frac{\partial\Delta\tilde{A}}{\partial\tau}\right]_{\Delta\rho,\xi}=c_t(\xi)\left[\frac{\partial\Delta\tilde{A}_r}{\partial t}\right]_{M,\xi}-c_\rho(\xi)d_1(\xi)\left[\frac{\partial\Delta\tilde{A}_r}{\partial M}\right]_{t,\xi}. \tag{A22}$$

4. Derived thermodynamic quantities

Pressure:

$$P=\frac{P_c(\xi)T}{T_c(\xi)}\left[\rho\left[\frac{\partial\Delta\tilde{A}_r}{\partial\rho}\right]_{\tau,\xi}-\Delta\tilde{A}_r(\tau,\rho,\xi)-\tilde{A}_0(\tau,\xi)\right]. \tag{A23}$$

Energy density:

$$\hat{u}=-RT_c(\xi)\left[\frac{\partial\hat{A}_{\text{eff}}}{\partial\tau}\right]_{\rho,\xi} \tag{A24}$$

$$=-P_c(\xi)\left[c_t(\xi)\left[\frac{\partial\Delta\tilde{A}_r}{\partial t}\right]_{M,\xi}-c_\rho(\xi)d_1(\xi)\left[\frac{\partial\Delta\tilde{A}_r}{\partial M}\right]_{t,\xi}+\sum_{j=1}^{4}j\tilde{A}_j(\xi)\tau^{j-1}+\frac{\rho}{\rho_c(\xi)}\sum_{j=1}^{5}j\tilde{\mu}_j(\xi)\tau^{j-1}\right]. \tag{A25}$$

Enthalpy density:

$$\frac{H}{V}=P/\rho+\hat{u}. \tag{A26}$$

[1] J. V. Sengers and J. M. H. Levelt Sengers, Annu. Rev. Phys. Chem. **37**, 189 (1986).
[2] P. C. Albright, Z. Y. Chen, and J. V. Sengers, Phys. Rev. B **36**, 877 (1987).
[3] Z. Y. Chen, P. C. Albright, and J. V. Sengers, Phys. Rev. A **41**, 3161 (1990).
[4] M. A. Anisimov and S. B. Kiselev, Sov. Tech. Rev. B Therm. Phys. **3** (2), 1 (1992).
[5] M. A. Anisimov, S. B. Kiselev, J. V. Sengers, and S. Tang, Physica A **188**, 487 (1992).
[6] Z. Y. Chen, A. Abbaci, S. Tang, and J. V. Sengers, Phys. Rev. A **42**, 4470 (1990).
[7] S. Tang and J. V. Sengers, J. Supercrit. Fluids **4**, 209 (1991).
[8] J. Luettmer-Strathmann, S. Tang, and J. V. Sengers, Fluid Phase Equilib. **75**, 39 (1992).
[9] M. E. Fisher, Phys. Rev. **176**, 257 (1968).
[10] R. B. Griffiths and J. C. Wheeler, Phys. Rev. A **2**, 1047 (1970).
[11] W. F. Saam, Phys. Rev. A **2**, 1461 (1970).
[12] M. A. Anisimov, A. V. Voronel, and E. E. Gorodetskii, Zh. Eksp. Teor. Fiz. **60**, 1117 (1971) [Sov. Phys. JETP **33**, 605 (1971)].
[13] S. S. Leung and R. B. Griffiths, Phys. Rev. A **8**, 2670 (1973).
[14] G. D'Arrigo, L. Mistura, and P. Tartaglia, Phys. Rev. A **12**, 2587 (1976).
[15] R. F. Chang and T. Doiron, Int. J. Thermophys. **4**, 337 (1983).
[16] M. R. Moldover and J. S. Gallagher, AIChE J. **24**, 268

(1978).
[17] M. R. Moldover and J. C. Rainwater, J. Chem. Phys. **88**, 7772 (1988).
[18] J. C. Rainwater, in *Supercritical Fluid Technology,* edited by J. F. Ely and T. J. Bruno (CRC, Boca Raton, FL, 1991), p. 57.
[19] J. J. Lynch and J. C. Rainwater, Fluid Phase Equilib. (to be published).
[20] J. M. H. Levelt Sengers, W. L. Greer, and J. V. Sengers, J. Phys. Chem. Ref. Data **5**, 1 (1976).
[21] J. M. H. Levelt Sengers and J. V. Sengers, in *Perspectives in Statistical Physics,* edited by H. J. Raveché (North-Holland, Amsterdam, 1981), p. 240.
[22] M. A. Anisimov, S. B. Kiselev, and I. G. Kostyukova, Teplofiz. Vys. Temp. **24**, 875 (1986) [High Temp. (USSR) **24**, 657 (1987)].
[23] M. A. Anisimov, S. B. Kiselev, and I. G. Kostukova, J. Heat Transfer **110**, 986 (1988).
[24] M. A. Anisimov, S. B. Kiselev, and S. E. Khalidov, Int. J. Thermophys. **9**, 453 (1988).
[25] S. B. Kiselev, I. G. Kostyukova, and A. A. Povodyrev, Int. J. Thermophys. **12**, 877 (1991).
[26] Z. Y. Chen, Ph.D. thesis, Institute for Physical Science and Technology, University of Maryland, 1988.
[27] J. C. Rainwater, *Vapor-Liquid Equilibrium of Binary Mixtures in the Extended Critical Region. I. Thermodynamic Model,* Natl. Inst. Stand. Technol Technical Note No. 1328 (U.S. GPO, Washington, DC, 1989).
[28] M. Ley-Koo and M. S. Green, Phys. Rev. A **23**, 2630 (1981).
[29] J. Souletie, H. Martin, and C. Tsallis, Europhys. Lett. **2**, 863 (1986).
[30] E. Carré and J. Souletie, J. Magn. Magn. Mater. **72**, 29 (1988).
[31] J. F. Nicoll, Phys. Rev. A **24**, 2203 (1981).
[32] J. F. Nicoll and P. C. Albright, Phys. Rev. B **31**, 4576 (1985).
[33] P. C. Albright, J. V. Sengers, J. F. Nicoll, and M. Ley-Koo, Int. J. Thermophys. 7, 75 (1986).
[34] J. C. Le Guillou and J. Zinn-Justin, Phys. Rev. B **21**, 3796 (1980).
[35] F. C. Zhang and R. K. P. Zia, J. Phys. A **15**, 3303 (1982).
[36] S. Tang, J. V. Sengers, and Z. Y. Chen, Physica A **179**, 344 (1991).
[37] A. J. Liu and M. E. Fisher, Physica A **156**, 35 (1989).
[38] K. E. Neuman and E. K. Riedel, Phys. Rev. B **30**, 6615 (1984).
[39] F. C. Zhang, Ph.D. thesis, Virginia Polytechnic Institute and State University, 1983.
[40] A. Michels and C. Michels, Proc. R. Soc. London Ser. A **153**, 201 (1935).
[41] A. Michels, C. Michels, and H. Wouters, Proc. R. Soc. London Ser. A **153**, 214 (1935).
[42] A. Michels, B. Blaisse, and C. Michels, Proc. R. Soc. London Ser. A **160**, 358 (1937).
[43] T. J. Edwards, Ph.D. thesis, University of Western Australia, 1984.
[44] A. Michels and S. R. de Groot, Appl. Sci. Res. A **1**, 94 (1948).
[45] D. R. Douslin and R. H. Harrison, J. Chem. Thermodyn. **5**, 491 (1973).
[46] H. M. Roder, J. Res. Natl. Bur. Stand. Sec A **80**, 739 (1976).
[47] J. Luettmer-Strathmann, S. Tang, and J. V. Sengers, J. Chem. Phys. **97**, 2705 (1992).
[48] D. G. Friend, H. Ingham, and J. F. Ely, J. Phys. Chem. Ref. Data **20**, 275 (1991).
[49] N. G. Shmakov, Teplofiz. Svoista Veshchestv Mater. **7**, 155 (1973).
[50] L. A. Weber, Int. J. Thermophys. **13**, 1011 (1992).
[51] P. C. Albright, T. J. Edwards, Z. Y. Chen, and J. V. Sengers, J. Chem. Phys. **87**, 1717 (1987).
[52] S. B. Kiselev, Teplofiz. Vys. Temp. **26**, 466 (1988) [High Temp. (USSR) **26**, 337 (1988)].
[53] G. X. Jin, S. Tang, and J. V. Sengers, Fluid Phase Equilib. **75**, 1 (1992).
[54] A. Abbaci, H. R. van den Berg, E. Sakonidou, and J. V. Sengers, Int. J. Thermophys. **13**, 1043 (1992).
[55] G. J. Sherman, J. W. Magee, and J. F. Ely, Int. J. Thermophys. **10**, 47 (1989).
[56] J. W. Magee, J. A. Howley, and J. F. Ely, Gas Processors Association Research Report RR135 (1992).
[57] N. E. Khazanova, L. S. Lesnevskaya, and A. V. Zakharova, Khim. Promst. (Moscow) **42**, 364 (1966).
[58] K. Ohgaki and T. Katayama, Fluid Phase Equilib. **1**, 27 (1977).
[59] J. C. Rainwater (private communication).
[60] M. A. Anisimov and J. V. Sengers, Phys. Lett. A (to be published).
[61] C. J. Wormald (private communication).

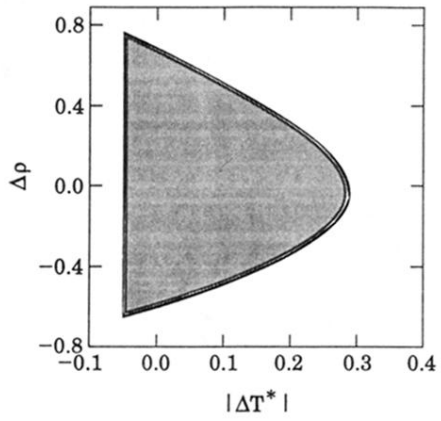

FIG. 1. Range of validity of the crossover free-energy density as a function of $\Delta T^* = (T - T_c)/T_c$ and $\Delta\rho = (\rho - \rho_c)/\rho_c$.